Progress in PHOTOVOLTAICS

PROGRESS IN PHOTOVOLTAICS: RESEARCH AND APPLICATIONS
Prog. Photovolt: Res. Appl. (2013)
Published online in Wiley Online Library (wileyonlinelibrary.com). DOI: 10.1002/pip.2426

RESEARCH ARTICLE

Comparative analysis of the outdoor performance of a dye solar cell mini-panel for building integrated photovoltaics applications

Cristina Cornaro[1,2]*, Simona Bartocci[1], Davide Musella[2], Cecilia Strati[2], Alessandro Lanuti[2,3], Simone Mastroianni[2,3], Stefano Penna[4], Andrea Guidobaldi[2,3], Fabrizio Giordano[2,3], Eleonora Petrolati[4], Thomas M. Brown[2,3,4], Andrea Reale[2,3,4] and Aldo Di Carlo[2,3,4]

[1] Department of Enterprise Engineering, University of Rome Tor Vergata, Via del Politecnico, 1 00133 Rome, Italy
[2] Centre for Hybrid and Organic Solar Energy (CHOSE), University of Rome Tor Vergata, Via del Politecnico, 1 00133 Rome, Italy
[3] Department of Electronic Engineering, University of Rome Tor Vergata, Via del Politecnico, 1 00133 Rome, Italy
[4] Dyepower Consortium, Viale Castro Pretorio, 122, 00185 Rome, Italy

ABSTRACT

New generation photovoltaic (PV) devices such as polymer and dye sensitized solar cells (DSC) have now reached a more mature stage of development, and among their various applications, building integrated PVs seems to have the most promising future, especially for DSC devices. This new generation technology has attracted an increasing interest because of its low cost due to the use of cheap printable materials and simple manufacturing techniques, easy production, and relatively high efficiency. As for the more consolidated PV technologies, DSCs need to be tested in real operating conditions and their performance compared with other PV technologies to put into evidence the real potential. This work presents the results of a 3 months outdoor monitoring activity performed on a DSC mini-panel made by the Dyepower Consortium, positioned on a south oriented vertical plane together with a double junction amorphous silicon (a-Si) device and a multi-crystalline silicon (m-Si) device at the ESTER station of the University of Rome Tor Vergata. Good performance of the DSC mini-panel has been observed for this particular configuration, where the DSC energy production compares favorably with that of a-Si and m-Si especially at high solar angles of incidence confirming the suitability of this technology for the integration into building facades. This assumption is confirmed by the energy produced per nominal watt-peak for the duration of the measurement campaign by the DSC that is 12% higher than that by a-Si and only 3% lower than that by m-Si for these operating conditions. Copyright © 2013 John Wiley & Sons, Ltd.

KEYWORDS

DSC; PV modules; BIPV; outdoor monitoring; performance

***Correspondence**

Cristina Cornaro, Department of Enterprise Engineering, University of Rome Tor Vergata, Via del Politecnico, 1 00133 Rome, Italy.
E-mail: cornaro@uniroma2.it

Received 1 February 2012; Revised 12 July 2013; Accepted 30 August 2013

1. INTRODUCTION

The importance of renewable energy integration on buildings is becoming stronger with the passing of time. Building integrated photovoltaics (BIPV) [1] began as a way to explore new technical solutions to integrate conventional building materials into roof, skylights, or facades. This background leads the research to concentrate on the real performance of PV devices that can be used for integration such as thin film amorphous silicon (a-Si) or the new emerging technology of dye sensitized solar cell (DSC) panels.

During the last 10 years, many papers on outdoor measurements were published all over the world, but contributions related to the Mediterranean area are still few, with the exception of Spain. In particular, some works concentrated on copper indium selenide (CIS) and amorphous silicon (a-Si) devices with different kind of junctions (see Ref. [2], just to cite an example) and many others on CIS, amorphous, multi-crystalline (m-Si), and crystalline silicon devices comparison, which focused on the behavior of power production versus solar irradiance (such as the results of the PV-Compare European project [3]). Moreover, regarding DSCs [4], few works on outdoor monitoring could be found in the literature. At the Fraunhofer Institute, outdoor test results on a glass facade prototype (70 × 200 cm) consisting of 10 modules (30 × 30 cm) were presented by Hinsch *et al*. [5]. Tests were carried out during 2 weeks of July and 2 weeks of October 2007. Later, Beucker *et al*. [6] illustrated the capability of the upgraded prototype from Fraunhofer, made up of modules of 60 × 100 cm in size. Zardetto *et al*. compared the diurnal performance of flexible curved devices with respect to flat ones [7]. Toyoda *et al*. [8] presented an outdoor performance of large scale DSC modules made up of 64 series-connected DSC cells, tested for half a year. More recently, Songyuan Dai *et al*. [9] presented a 354 day long monitoring of the Isc and Voc on a 500 W DSC primary power station. The longest outdoor monitoring activity on DSC was carried out by Kato *et al*. [10], which fabricated their own DSC module and tested it for 2.5 years, presenting the mean monthly values of Isc, Voc, FF, and efficiency versus irradiance and time. Lastly, Mastroianni *et al*. [11] presented a long-term life test (3200 h) on large-area DSCs performed under both outdoor and indoor conditions, with different cells' working points (open-circuit voltage and near the maximum power point) and cells' orientation (vertically and horizontally oriented cells).

In addition, the influence of meteorological parameters changes on DSC and organic devices have still not been investigated enough: Katz *et al*. [12], for example, performed 32 subsequent days test on polymeric devices from March to April with a peak temperature of 45°C and pointed out that Isc goes down with the passing of time (the opposite for Voc). Later, Hauch *et al*. [13] carried out a 1 year outdoor exposure of a flexible organic module at 42.6°N, in the USA, correlating the results with an accelerated indoor test under 1 sun at 65°C for 1200 h. Cornaro *et al*. [14,15] made the first considerations on the impact of meteorological parameters on DSC cells. To the authors' knowledge, no comparative evaluation of DSC panels with regard to other PV technologies for a reasonable period of time has yet been performed, and furthermore, no vertical plane configuration suitable for BIPV applications has been investigated.

The present work wants to be a first contribution to these issues. A 3 month continuous outdoor monitoring activity was carried out on a DSC mini-panel manufactured by Dyepower, a consortium that includes several partners, among them are a leading company for glass facades, Permasteelisa, an energy company, ERG Renew, and the Universities of Roma Tor Vergata, Ferrara, and Torino. Dyepower was established to pursue the industrialization of DSC technology for BIPV applications and in particular for the development of a pilot line for the production of DSC PV glass facades. The device, named DSC in the paper, was tested against double junction a-Si and m-Si panels, to evaluate the behavior of these devices mounted on a vertical plane (for facade applications), facing south, and to compare the real performance when the solar radiation is not at optimal incidence, and under different operative temperature conditions.

2. EXPERIMENTAL

This work aims to give the results of outdoor tests carried out at ESTER, solar and meteorological station located on the rooftop of the engineering building of the University of Rome Tor Vergata (Lat. 41°51′28.17″, Lon. 12°37′ 23.9″). A dedicated stand suitably designed for BIPV applications was built in order to give the maximum flexibility to the research.

The frame, shown in Figure 1, can be rotated in every position on the azimuth plane and is equipped with an integrated compass and a sensor to level it on the horizontal plane. Its tilt angle can be varied from 0° to 90° using two telescopic shafts connected through bolts. This type of control is useful for any outdoor test in order to give results that are as near as possible to the real performance of PV devices integrated on various buildings facades and roofing configurations. The performance of the double junction a-Si frameless panel from EPV Solar, model EPV-50, with a nominal peak power of 50 W, named a-Si, and the DSC mini-panel were investigated from August 11 to October 22, 2011 and compared with the performance of a m-Si panel from Helios Technology (Padua, Italy), model HMA214P, with a nominal peak power of 214 W, named m-Si, each of them arranged on the dedicated stand in a vertical configuration (0° tilt), facing south. The a-Si module was exposed to outdoor conditions for 18 months prior to the present test, and a 4 months period was needed for module stabilization [16]. A seasonal

Figure 1. View of the photovoltaic modules arranged on the dedicated frame and the detail of the dye sensitized solar cells (DSC) mini-panel.

Prog. Photovolt: Res. Appl. (2013) © 2013 John Wiley & Sons, Ltd.
DOI: 10.1002/pip

variation in performance [17] was observed, and it will be described in the Section 3.

The aforementioned modules were not intentionally chosen for the test comparison, but they were available at the laboratory at the time of the monitoring campaign. Moreover, both the m-Si and a-Si used are not to be considered as fully representative of the respective technologies, and also, they are not the best performing modules of their category. Nonetheless, their behavior with respect to the environmental parameters and the configuration tested can be considered representative of the technology.

The monitoring campaign can be considered as a preliminary test, and it was conducted for a short period of time because the DSC panels, in general, still show some durability problems related to the sealing methodology [18]. However, because the test is intended as a comparative analysis, the duration and season of the comparison are not of direct significance for the presented results.

The DSC panel, shown in Figure 1, consisted of four electrically separated mini-panels; only the circled mini-panel in the figure was continuously monitored. The tested device was realized by series connection of three DSC modules. Each DSC module presents 13 semitransparent cells connected in series following the so-called integrated Z layout. DSC cells are fabricated utilizing fluorine-doped tin oxide coated glass substrates, a semitransparent TiO_2 layer, N719 dye, a Pt-based counter electrode, and an iodide/tri-iodide liquid electrolyte [19]. The mini-panel is assembled between external standard soda-lime glasses through a lamination procedure.

The DSC mini-panel has an active area of 511.7 cm^2. The active area used for the efficiency calculation includes only the surface occupied by the DSC cells strips that is approximately the 73% of the total surface of the mini-panel.

Electrical performance was recorded before the start of the outdoor test. Figure 2 shows the *I–V* curve of the mini-panel. Table I presents the technical specifications of the three devices provided by the manufacturers under standard test conditions (STC). For STC, an irradiance of 1000 W/m^2, a temperature of the module of 25°C, and an air mass of 1.5 are intended.

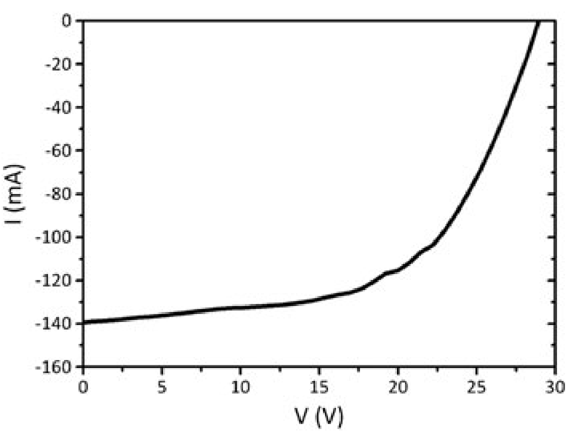

Figure 2. *I–V* curves of the dye sensitized solar cells mini-panel after the lamination procedure.

The panels were kept at the maximum power point by a suitable electronic device (MPPT 3000, ISAAC SUPSI, Lugano CH), and every minute, the electrical and meteorological parameters were collected by a dedicated data logger. Irradiance was measured on the same plane of the modules and was defined as "plane of array irradiance" (*Gpoa*). Besides, every 10 min, the *I–V* curves were traced for all panels. Uncertainties for all the measured parameters at the ESTER station were evaluated and are listed elsewhere [20].

Data were stored in a dedicated database, and a purposely made software called Noria (ESTER Laboratory, Rome, Italy), which can be implemented by a specific query from the user, was used for data extraction. Downloaded data were then cleaned by a filtering procedure that was implemented in MATLAB software (Mathworks Inc., Natich, MA, USA), in order to eliminate those values coming from system faults and values that were out of the physical range limits [16].

The test was designed for the double purpose of comparing the performance of the three devices in the vertical configuration and of checking their stability. For this reason, every 15 days, during the continuous monitoring, the frame was tilted to optimal tilt (normal incidence at noon) to measure the *I–V* curves of the devices in outdoor conditions [21]. Peak power of the three modules was then evaluated by translating the curves to STC using the Blaesser method [22] and comparing them with the nominal values provided by the manufacturer for the various optimal tilt periods.

3. RESULTS

The results of the monitoring campaign will be presented in four separate sections. The first section will illustrate the climatic characterization at the site for the period of interest. In the second section, considerations on the stability of the devices are addressed. The third section will show and analyze the typical daily trends of the performance of the different technologies for a sunny day representative of the summer period and a sunny day representative of the autumn period. Lastly, final considerations on the performance of the various technologies for the period of test are made.

3.1. Climatic characterization

Weather data analysis was carried out for the 3 months of monitoring, focusing on irradiance availability and ambient temperature trends. The irradiance resource for the location was evaluated in terms of frequency distribution of the incoming energy and cloud ratio (*CR*).

The *CR* gives an indication of the strength of diffuse irradiance at a particular time. It is defined as the ratio of the horizontal diffuse irradiance over the global horizontal irradiance, and it gives an indication of the cloud coverage. It ranges from 0 to 1 with 0 meaning very clear sky and 1 meaning overcast sky. *CR* was calculated on a daily basis, and the *CR* range was divided into five classes: "very clear sky" with *CR*

Table I. Characteristics at STC of the PV devices under test.

Manufacturer	Model	*Pn* (W)	*Im* (A)	*Vm* (V)	*Isc* (A)	*Voc* (V)	*FF* (%)	η(%)
Dyepower (DSC)	DP-Z-2.5W	2.32	0.112	20.72	0.139	28.95	57.49	4.50
Helios Technology (m-Si)	HMA214P	214	7.460	28.69	8.030	36.63	72.75	13.1
EPV Solar (a-Si)	EPV-50	50	1.12	45.00	1.410	60.00	53.45	5.32

STC, standard test conditions; PV, photovoltaic; DSC, dye sensitized solar cells; m-Si, multi-crystalline silicon; a-Si, amorphous silicon.

ranging from 0 to 0.2, "clear sky" with *CR* ranging from 0.2 to 0.4, "partly cloudy sky" with *CR* ranging from 0.4 to 0.6, "cloudy sky" with *CR* ranging from 0.6 to 0.8, and "heavy cloudy sky" with *CR* ranging from 0.8 to 1.0. For each of the classes, the daily *CR* frequency was evaluated.

Figure 3 represents the five *CR* classes frequency during the period. It can be observed that a favorable weather, with high percentage of clear sky, was observed during the test period.

Ambient temperature and irradiance were elaborated to obtain the irradiation and the average ambient temperature evaluated at various plane of the array irradiance classes, as shown in Figure 4. In-plane irradiance (*Gpoa*) was divided into 10 W/m^2 intervals, and for each interval, the solar irradiation (*I*) and ambient temperature (*Tamb*) were calculated.

The graph shows a higher energy availability for medium irradiances with a peak around 500 W/m^2. This is due to the fact that in the months of test, high sun elevation and high angles of incidence are expected on the vertical plane position. Secondary peaks (e.g., the one at 700 W/m^2) are due to progressively smaller angles of incidence (due to the varying position of the sun) that increase the energy contribution to high irradiance intensities.

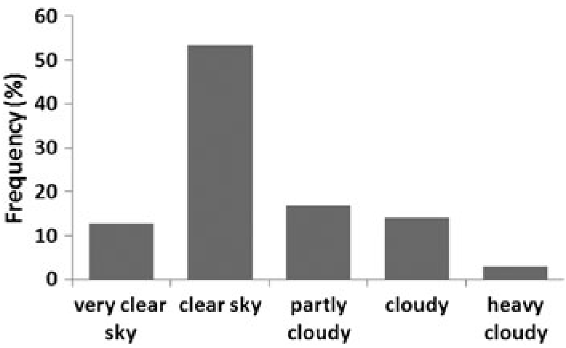

Figure 3. Cloud ratio frequency evaluated for the period of test.

Also, temperature distribution on the back of the module was evaluated at a different plane of the array irradiance classes. Figure 5 shows the trends for three monitored panels.

The DSC panel temperature is lower than that of the a-Si and m-Si devices for high irradiance intensities. This is due to its particular construction technology. a-Si and m-Si modules follow approximately the same trend.

3.2. Stability

As already mentioned, the devices were also checked for their peak power values and stability in outdoor conditions, during the months of operation. Every 15 days, the frame was tilted at normal incidence at noon, and various *I–V* curves were measured. For each device, the measured curves were translated to STC, and for each period, the curves parameters were calculated as the average of the values obtained from the various measured curves. Irradiance stability was accurately checked during data acquisition considering only the *I–V* curves traced while the irradiance stability was within ±1% in a time interval of 2 min.

Figure 6 shows the calculated *Pmax* at STC normalized for the nominal (manufacturer) maximum power (*Pmax, rel*) and for the *Pmax* at STC measured at the beginning of the campaign (*Pin*) versus time for the three devices. From the *Pmax,rel* trend, the differences between nominal

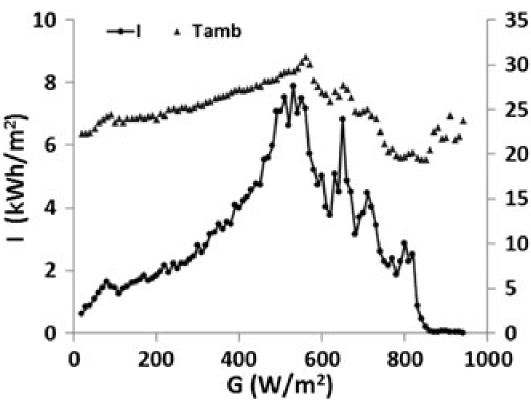

Figure 4. Irradiation (*I*) and average ambient temperature (*Tamb*) measured at different plane of array irradiance classes.

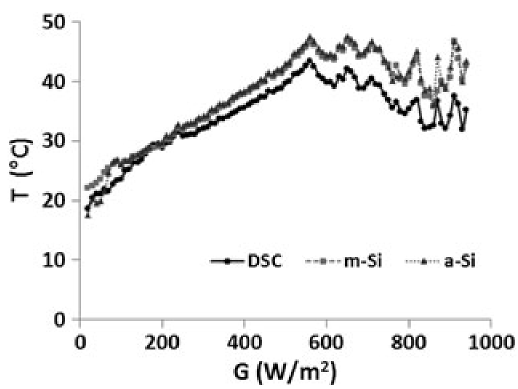

Figure 5. Average back of the module temperatures evaluated at different plane of array irradiance classes.

Prog. Photovolt: Res. Appl. (2013) © 2013 John Wiley & Sons, Ltd.
DOI: 10.1002/pip

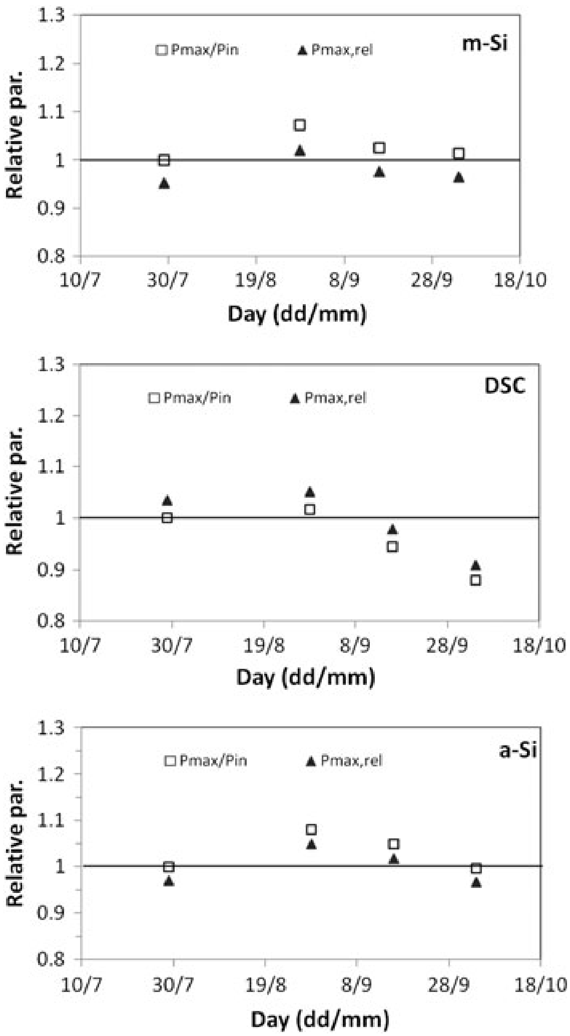

Figure 6. Variation of *Pmax* translated at standard test conditions (STC), normalized by the nominal (manufacturer) maximum power (*Pmax,rel*) and for the measured *Pmax* at STC obtained at the beginning of the campaign (*Pin*) versus time for the three devices during the period of test. DSC, dye sensitized solar cells.

and measured power can be quantified. The *Pmax*/*Pin* trend can be analyzed for the stability. From the data normalized to the nominal peak power, a fluctuation within ±5% can be observed for m-Si and a-Si. As can be seen from Table II, nominal power is overestimated with respect to the measured average by approximately 2% for m-Si, while for a-Si, the two values are similar (within 0.16%). DSC shows a fluctuation of +5%/−10% with an average measured *Pmax* of 0.06% lower than that of the nominal.

As evidenced from the curve of *Pmax*/*Pin*, the polycrystalline and amorphous devices show high stability during the measurement period. The DSC, instead, exhibits a loss of in-peak power of approximately 0.2 W over the period.

Table II. Difference between nominal peak power (*Pn*) and measured average peak power (*Pavg*) for the devices.

Manufacturer	*Pn* (W)	*Pavg* (W)	(*Pn* − *Pavg*)/*Pn* (%)
Dyepower (DSC)	2.32	2.305	0.60
Helios Technology (m-Si)	214	209.4	2.00
EPV Solar (a-Si)	50	50.08	−0.16

DSC, dye sensitized solar cells; m-Si, multi-crystalline silicon; a-Si, amorphous silicon.

3.3. Outdoor performance on a sunny day

As a first step, we compared the outdoor daily performance of DSC module to the outdoor performance of commercial a-Si and m-Si that were installed on a vertical plane at the same test site. The comparison of the modules' data is shown in Figure 7 for a sunny day in August and in Figure 8 for a sunny day in October.

Comparisons are made in terms of efficiency and fill factor. The efficiency was normalized with respect to the magnitude value at noon.

Although the absolute STC efficiency for the m-Si device is definitely higher (13.1%) than for the DSC (4.5%) (comparable instead with a-Si (5.3%)), it can be observed that for low irradiance, a good advantage of the DSC panel relative efficiency is shown during the whole length of the test period. The trend of the relative efficiency is not symmetrical for all panels, in particular for DSC. This is due to thermal effects and to the particular operating condition, such as incident useful irradiance. As observed for the m-Si modules, high temperature reduces DSC module performance, and this is the reason why the relative efficiency is higher during morning than during afternoon hours characterized by a higher average ambient temperature. Moreover, this asymmetrical trend of the efficiency is more pronounced in the month of October (Figure 8(a)) for all the modules' technologies. This effect could be related to the higher temperature difference between morning and afternoon for the period.

Besides, the increased efficiency of DSC panel for low irradiance levels could be due to its spectral response that is more shifted towards short wavelengths, so that DSC should be more sensitive to diffuse light which is characterized by a blue shifted spectrum and it is predominant at the beginning and at the end of the day. Because m-Si has a broader spectral response, blue shifts do not significantly affect its behavior. a-Si, instead, should behave more like DSC because of its spectral response, but we did not observe this phenomenon for this configuration. Furthermore, early in the morning and late in the afternoon, the angles of incidence of the sun rays are far from normal incidence, and a clear systematic improvement of efficiency in angle has been reported in a recent study [23].

In August (Figure 7(a)), at the end of the day, a small peak in the relative efficiency trend, which is more evident for the m-Si module, is observed. This is probably due to mismatch between the angle of view of the planes of the modules' planes and the angle of view of the integrating sphere of

DOI: 10.1002/pip

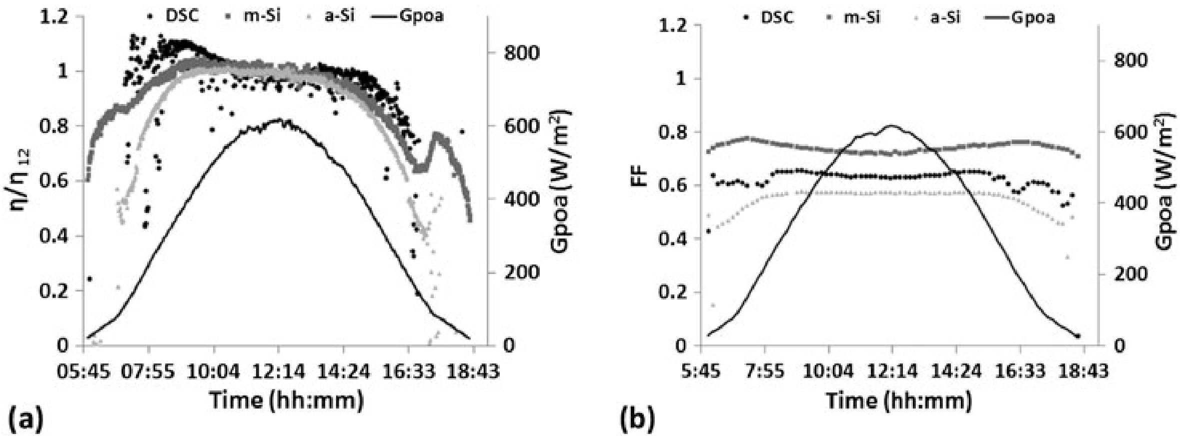

Figure 7. Performance of dye sensitized solar cells, multi-crystalline silicon, and amorphous silicon devices for a sunny day in August 2011: (a) relative efficiency and (b) fill factor.

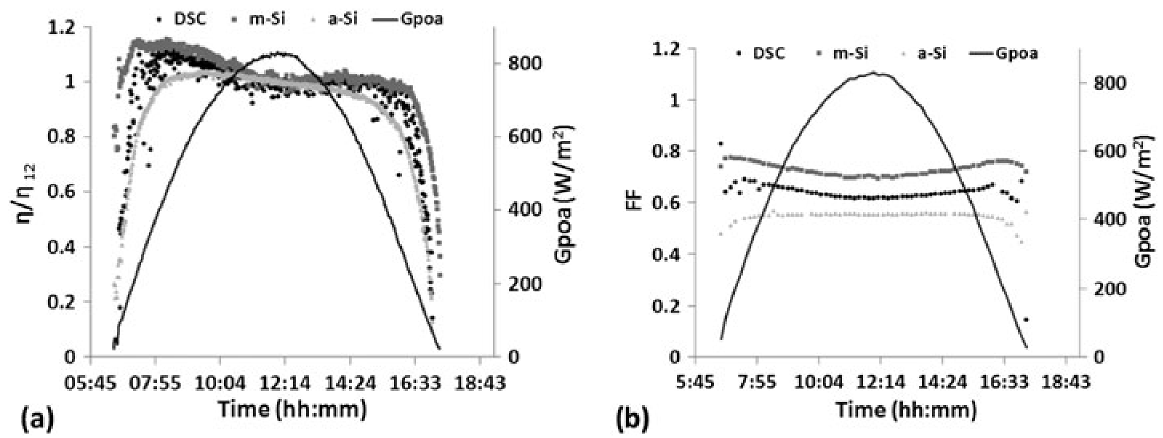

Figure 8. Performance of dye sensitized solar cells, multi-crystalline silicon, and amorphous silicon modules for a sunny day in October 2011: (a) relative efficiency and (b) fill factor.

the pyranometer, when the sun is low. In October, the small peak disappeared owing to running to the different seasonal solar path.

As it can be noted by Figures 7(b) and 8(b), the fill factor of the DSC module is higher than the one of the a-Si module and is better at low irradiance levels as is for the m-Si module. This confirms what has been observed by Hinsch *et al*. [5].

3.4. Energy yield and performance ratio

To evaluate the performance of PV modules of various technologies, a numbers of indices can be considered. The main index used in the absence of direct measurements on the module is the efficiency and power at STC. These conditions are considered as reference for the modules' energy yield evaluation. If one wants to evaluate and to compare the energy production of different modules of different power sizes, the energy yield is the suitable parameter to use. The energy yield (Y) is written as follows:

$$Y = \frac{E}{P_n} \quad [\mathrm{kWh/kW}] \tag{1}$$

where E is the electrical energy produced by the module in a defined time interval and P_n is the nominal peak power. This index can also be interpreted as the number of hours in which the PV modules work at their peak power value. Because the energy production is normalized to the module size, this index allows to compare PV devices of different peak power.

It is well known that the energy production of a PV module does not depend only on radiation intensity but also, to some extent, on the temperature of the module, on the variation of solar spectrum and also on other factors that do not strictly depend on the module itself. To take into account all these influences, another index called

Prog. Photovolt: Res. Appl. (2013) © 2013 John Wiley & Sons, Ltd.
DOI: 10.1002/pip

performance ratio (*PR*) is defined [24]:

$$PR = \frac{Y}{Y_r} \quad \text{with} \quad Y_r = \frac{I}{G_{STC}} \tag{2}$$

Yr is called the reference yield and is the ratio between the irradiation evaluated in the considered time interval and the irradiance at STC; it also represents the sun peak hours defined as the hours in which the in-plane irradiance has reached the 1000 W/m^2. The *PR* index can also be seen as the ratio of the real efficiency over the efficiency at STC, and for this reason, it measures how far the behavior of the module is with respect to its performance at STC. *PR* is used as a comparative performance parameter, however the variability of manufacturers' data with respect to variations in yield for a given module is not necessarily well represented by the manufacturer's numbers used for the PR evaluation. This effect could introduce a slight unreliability in the use of *PR* to compare different technologies.

For the DSC, m-Si, and a-Si modules, the daily yield was calculated for the whole test period normalizing the energy production by the nominal peak power (from the manufacturer) and is shown in Figure 9. As pointed out in the stability section and reported in Table II, the difference between the nominal power declared by the manufacturers and the measured average power for the period of test is almost the same for DSC and a-Si while it is approximately 2% for m-Si. However, these slight differences have been taken into account for each module and commented later on in the results analysis.

The missing data in the graphs are due to the days in which the modules were subjected to stability tests. An increasing trend in time of the yield for all modules can be noted, due to the decrease in the angle of incidence during the transition from summer to autumn. The fluctuations in the yield are due to the weather conditions represented, in Figure 10, by the *CR* and reference yield or peak sun hours. In fact, *CR* values near 1 are representative of bad weather conditions; therefore, less peak sun hours could be observed. *CR* values near 0 represent clear sky conditions with higher radiation intensities and consequently higher peak sun hours values.

From the comparative analysis among technologies, the DSC module shows excellent yield until the middle of September, comparable with the energy production of the m-Si module. In Figure 11, the trend of the *PR* for all the technologies is shown. The data used for the analysis allow to evaluate the *PR* with an uncertainty of ±5% essentially due to uncertainty in the irradiance measurement. As already mentioned, this index is slightly sensitive to irradiance variation and more dependent on secondary effects on the module performance such as temperature and angle of incidence.

The *PR* of the DSC and m-Si modules is higher than the *PR* of the a-Si module until the September 15. After that date, the DSC module seems to reach a stable phase characterized by an intermediate performance between that of m-Si and a-Si modules.

For the m-Si module, an increase of the *PR* from August to October is reported. This is due to the double favorable effect induced by the decreasing of the angle of incidence and by the module temperature, passing from summer to autumn. For the a-Si module, instead, a more stable trend is observed probably due to competitive contribution of temperature, annealing, spectrum, and angle of incidence effects. This is supported by an accurate analysis of previous long-term data that also evidenced a low temperature annealing effect with a maximum positive contribution exactly in the period between September and October [25].

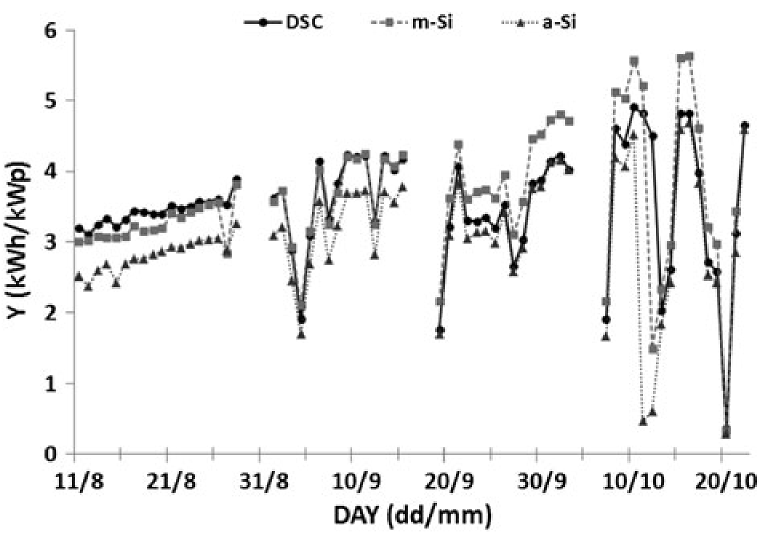

Figure 9. Daily yield calculated for dye sensitized solar cells, multi-crystalline silicon, and amorphous silicon modules.

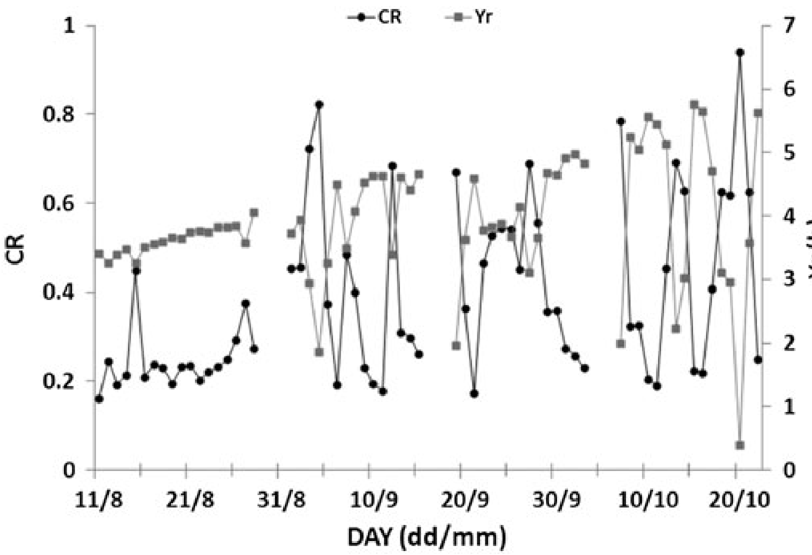

Figure 10. Daily cloud ratio (*CR*) and reference yield (*Yr*) for the period of test.

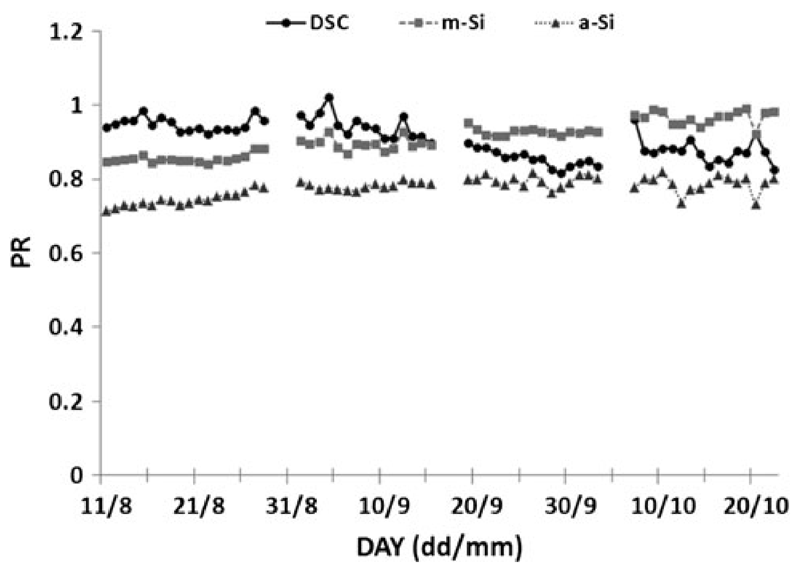

Figure 11. Daily performance ratio (*PR*) calculated for dye sensitized solar cells, multi-crystalline silicon, and amorphous silicon modules for the period of test.

To investigate the behavior of the three PV technologies on a monthly basis, the *PR* was evaluated and shown in Figure 12 for the monitoring period.

The optimum performance observed for DSC in comparison with a-Si and m-Si for the month of August is essentially related to the better response of the mini-panel to high solar angle of incidence on a vertical plane during summer and also to the minor sensitivity to the high temperature values experienced in August. The temperature dependence of the devices' performance was evaluated through the temperature coefficient for the power for the three technologies; for m-Si and a-Si, a value of −0.49%/°C and −0.19%/°C was declared from the manufacturer while for DSC, the same coefficient was directly evaluated from our data, which yielded a value of −0.39%/°C. This result explains why DSC has a better performance (*PR*) with respect to m-Si, considering that *PR* is mostly influenced by temperature. The a-Si appears less influenced by the higher summer temperatures, as expected, but surprisingly, it seems to suffer for the particular vertical plane configuration. Indeed, looking at the following months, only a slight increase in *PR* for a-Si is observed owing to the double effect of temperature and variation of angle of incidence, while for m-Si, the more evident increase is related to the higher sensitivity of the technology to the aforementioned parameters.

DOI: 10.1002/pip

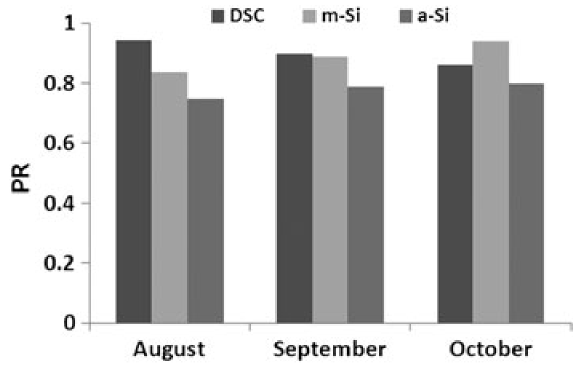

Figure 12. Monthly performance ratio (*PR*) calculated for dye sensitized solar cells, multi-crystalline silicon, and amorphous silicon modules for the period of test.

Table III. Performance of the three technologies for the period of test.

Period	Type	Minutes of operation	I (kWh/m^2)	PR (%)	Y (kWh/kWp)	η (%)	$Tamb$ (°C)	$Tmod$ (°C)	$Tmod\ max$ (°C)
August 11 to	DSC	38455	269	89.3	240.28	4.04	26	34.90	53.0
October 22, 2011	m-Si	48170	280	88.5	248.27	11.6	26	35.01	57.6
	a-Si	41410	272	77.5	210.76	4.12	26	38.05	57.9

DSC, dye sensitized solar cells; m-Si, multi-crystalline silicon; a-Si, amorphous silicon.

Table III summarizes the performance of the three technologies for the period of interest. Reported temperature values are the average of the data collected during the time of the devices' operation (i.e., diurnal data) for the period of the campaign (August 11 to October 22, 2011); *Pr*, *Y*, and η were evaluated by integrating the generated power and the solar irradiance over the whole period of the test. Because of the data filtering procedure, the period of operation of the three panels is not the same, with 25% more minutes of activity for m-Si with respect to DSC. Nevertheless, a difference in yield of only 3% is observed for the two technologies normalizing for the nominal peak power, increasing to 5% if the normalization is made using the measured average peak power, indicating an overall better performance of DSC. The double junction a-Si panel appears to be the worst performing device with a percentage difference of *Y* with respect to DSC of 12% (nominal peak power normalization) that reaches 14% normalizing the produced energy by the average measured peak power.

4. CONCLUSIONS

A 3 month outdoor monitoring campaign, started in August 2011 and ended in October 2011, was carried out on a DSC mini-panel, an a-Si device, and an m-Si device with the objective to better understand their behavior and to compare performance in real operating conditions suitable for integration into building facades (vertical position). It has to be pointed out that the results obtained cannot be extended to every device of the considered technologies because differences can be encountered among panels of the same technology but of different manufacturers. Moreover, a longer monitoring period should be considered to have an idea of possible seasonal effects. However, some useful information could be derived from the outdoor experimental activity here presented. The DSC performance appears very encouraging with a *PR* calculated using the energy collected during the whole period of 89.3% to be compared with a value of 88.5% for m-Si and a much lower 77.5% for a-Si, for the vertical plane configuration, facing south. Also, for the same configuration, the energy per measured average watt-peak produced by DSC is 12% higher than that by a-Si and only 3% lower than that by m-Si. From the comparative analysis among the modules of different technologies, the DSC panel shows high yield from the beginning of the test until the middle of September, comparable with the energy production of the m-Si module. Optimum performance observed for DSC in comparison with a-Si and m-Si for the month of August has been related to the better response of the mini-panel to high solar angle of incidence on a vertical plane during summer and also to it being less sensitive to the high temperature values experienced in August with respect to the m-Si device. On the whole, for the time period analyzed, DSC shows a better performance with respect to the double junction a-Si module tested and a comparable behavior with the m-Si panel.

NOMENCLATURE

Symbol	Quantity	SI unit
CR	Cloud ratio	Dimensionless
FF	Fill factor	Dimensionless
Gpoa	Plane of the array irradiance	W/m^2
I	Irradiation	kWh/m^2
Pavg	Average peak power	W
Pin	Peak power measured at the beginning of the campaign	W
Pmax	Maximum (peak) power translated at STC	W
Pmax,rel	Maximum power normalized to *Pn*	Dimensionless
Pn	Nominal peak power (manufacturer)	W
PR	Performance ratio	Dimensionless
Tamb	Ambient temperature	°C
Tmod	Module temperature	°C
Y	Yield	kWh/kWp
Yr	Reference yield	h
η	Efficiency	%
η_{12}	Efficiency at 12:00 PM	%

REFERENCES

1. IEA – International Energy Agency. Potential for building integrated photovoltaics. Report IEA PVPS Task 7, NET Ltd., 2002, St. Ursen, Switzerland.
2. Gottschalg R, del Cueto JA, Betts TR, Infield DG. Seasonal performance of a-Si single- and multijunction modules in two locations. Photovoltaic Specialists Conference, 2005. Conference Record of the Thirty-first IEEE.
3. Jardine CN, Conibeer GJ, Lane K. PV-COMPARE: direct comparison of eleven PV technologies at two locations in northern and southern Europe. Seventeenth EU PVSEC, 2001.
4. O'Regan B, Grätzel M. A low-cost, high-efficiency solar cell based on dye-sensitized colloidal TiO2 films. *Nature* 1991; **353**: 737.
5. Hinsch A, Brandt H, Veurman W, Hemming S, Nittel M, Würfel U, Putyra P, Lang-Koetz C, Stabe M, Beucker S, Fichter K. Dye solar modules for façade applications: recent results from project Color Sol. *Solar Energy Materials & Solar Cells* 2009; **93**: 820–824.
6. Beucker S, Hinsch A, Brandt H, Veurman W, Flarup Jensen K, Lang-Koetz C, Stabe M. Scaling-up of glass based DSC-modules for applications in building integrated photovoltaics, 34th IEEE Photovoltaic Specialists Conference (PVSC), 2009.
7. Zardetto V, Mincuzzi G, De Rossi F, Di Giacomo F, Reale A, Di Carlo A, Brown TM. Outdoor and diurnal performance of large conformal flexible metal/plastic dye solar cells. (manuscript accepted), Applied Energy.
8. Toyoda T, Sano a T, Nakajima a J, Doi a S, Fukumoto S, Ito A, Tohyamaa T, Yoshida M, Kanagawa T, Motohiro T, Shiga T, Higuchi K, Tanaka H, Takeda Y, Fukano T, Katoh N, Takeichi A, Takechi K, Shiozawa M. Outdoor performance of large scale DSC modules. *Journal of Photochemistry and Photobiology A: Chemistry* 2004; **164**: 203–207.
9. Dai S, Weng J, Sui Y, Chen S, Xiao S, Huang Y, Kong F, Pan X, Hu L, Zhang C, Wang K. The design and outdoor application of dye-sensitized solar cells. *Inorganica Chimica Acta* 2008; **361**: 786.
10. Kato N, Takeda Y , Higuchi K, Takeichi A, Sudo E, Tanaka H, Motohiro T, Sano T, Toyoda T. Degradation analysis of dye-sensitized solar cell module after long-term stability test under outdoor working condition. *Solar Energy Materials & Solar Cells* 2009; **93**: 893–897.
11. Mastroianni S, Lanuti A, Penna S, Reale A, Brown TM, Di Carlo A, Decker F. Physical and electrochemical analysis of an indoor–outdoor ageing test of large-area dye solar cell devices. *ChemPhysChem* 2012; **13**(12): 2925–2936.
12. Katz EA, Gevorgyan S, Orynbayev MS, Krebs FC. Outdoor testing and long-term stability of plastic solar cells. *The European Physical Journal Applied Physics* 2006; **36**: 307–311.
13. Hauch JA, Schilinsky P, Choulis SA, Childers R, Biele M, Brabec CJ. Flexible organic P3HT:PCBM bulk-heterojunction modules with more than 1 year outdoor lifetime. *Solar Energy Materials & Solar Cells* 2008; **92**: 727–731.
14. Cornaro C, Spena A, Brown TM, Di Carlo A, Reale A. The impact of meteorological parameters on the performance of dye-sensitized solar cells. Proceedings of the 33rd IEEE PV specialists Conference, San Diego (CA), May, 11–16 2008.
15. Cornaro C, Spena A, Brown TM, Di Carlo A, Reale A, Martella S. Outdoor characterization of dye solar cells: first results. Proceedings of the 24th European Photovoltaic Solar Energy Conference and Exhibition, September 21–24, 2009.
16. Cornaro C, Musella D. Comparative analysis of crystalline and double-junction amorphous silicon modules performance in outdoor conditions. *Journal of Solar Energy Engineering* 2013; **135**(3).
17. Ruther R, Livingstone J. Seasonal variations in amorphous silicon solar module outputs and thin film characteristics. *Solar Energy Materials and Solar Cells* 1994; **36**: 29–43.
18. Ileperuma OA. Gel polymer electrolytes for dye sensitized solar cells: a review. *Materials Technology: Advanced Performance Materials* 2013; **28**(1–2): 65–70(6).
19. Giordano F, Petrolati E, Brown TM, Reale A, Di Carlo A. Series-connection designs for dye solar cell

 Prog. Photovolt: Res. Appl. (2013) © 2013 John Wiley & Sons, Ltd.
DOI: 10.1002/pip

modules. *Transactions On Electron Devices* 2011; **58**: 2759. DOI: 10.1109/TED.2011.2158216
20. Spena A, Cornaro C, Intreccialagli G, Chianese D. Data validation and uncertainty evaluation of the ESTER outdoor facility for testing of photovoltaic devices. Proceedings of the 24th European Photovoltaic Solar Energy Conference and Exhibition, Hamburg, Germany, September 21–24, 2009.
21. EN 60904–1. Measurement of photovoltaic current–voltage characteristics.
22. Blaesser G, Zaaiman W. On-site power measurement on large PV-arrays. 10th European Solar Energy Conference, Lisbon, 1991.
23. D'Ercole D, Dominici L, Brown TM, Michelotti F, Reale A, Di Carlo A. Angular response of dye solar cells to solar and spectrally resolved light. *Applied Physics Letters* 2011; **99**: 213301. DOI: 10.1063/1.3663973
24. Marion B. Adelstein J, Boyle K, Hayden H, Hammond B, Fletcher T, Canada B, Narang D, Shugar D, Wenger H, Kimber A, Mitchell L, Rich G, Townsend T. Performance parameters for grid-connected PV systems. Proceedings of the 31st IEEE Photovoltaics Specialists Conference, Lake Buena Vista, Florida, January 3–7, 2005.
25. Pierro M, Bucci F, Cornaro C. Full characterization of PV modules in real operating conditions: theoretical model, measurement method and results Submitted for publication to Progress in Photovoltaics: Research and Applications, 2013.